Enhanced genetic analysis of type 1 diabetes by selecting variants on both effect size and significance, and by integration with autoimmune thyroid disease

Daniel J. M. Crouch[1], Jamie R.J. Inshaw[1], Catherine C. Robertson[2], Jia-Yuan Zhang[1], Wei-Min Chen[2,3], Suna Onengut-Gumuscu[2,3], Antony J. Cutler[1], Carlo Sidore[4], Francesco Cucca[4], Flemming Pociot[5,6,7], Patrick Concannon[8,9], Stephen S. Rich[2,3], John A. Todd[1*]

[1]JDRF/Wellcome Diabetes and Inflammation Laboratory, Wellcome Centre for Human Genetics, Nuffield Department of Medicine, NIHR Oxford Biomedical Research Centre, University of Oxford, Oxford, United Kingdom
[2]Center for Public Health Genomics, University of Virginia, Charlottesville, Virginia, USA
[3]Department of Public Health Sciences, University of Virginia, Charlottesville, Virginia, USA
[4]Institute for Research in Genetics and Biomedicine (IRGB), Sardinia, Italy
[5]Department of Pediatrics, Herlev University Hospital, Copenhagen, Denmark
[6]Institute of Clinical Medicine, Faculty of Health and Medical Sciences, University of Copenhagen, Copenhagen, Denmark
[7]Type 1 Diabetes Biology, Department of Clinical Research, Steno Diabetes Center Copenhagen, Gentofte, Denmark
[8]Department of Pathology, Immunology, and Laboratory Medicine, University of Florida, Gainesville, Florida, USA
[9]Genetics Institute, University of Florida, Gainesville, Florida, USA

*Corresponding author:
John Todd (jatodd@well.ox.ac.uk)
Wellcome Centre for Human Genetics
Nuffield Department of Medicine
NIHR Oxford Biomedical Research Centre
University of Oxford

Abstract

For polygenic traits, associations with genetic variants can be detected over many chromosome regions, owing to the availability of large sample sizes. The majority of variants, however, have small effects on disease risk and, therefore, unraveling the causal variants, target genes, and biology of these variants is challenging. Here, we define the Bigger or False Discovery Rate (BFDR) as the probability that either a variant is a false-positive or a randomly drawn, true-positive association that exceeds it in effect size. Using the BFDR, we identify new variants with larger effect associations with type 1 diabetes and autoimmune thyroid disease.

Introduction

Most genome-wide association study (GWAS) associations have small effects on phenotypes, with the genetic risk for common diseases distributed across hundreds of loci, mostly with common alleles[1]. Interpretation of the biological effects of these variants, and establishment of which are causal, either statistically (fine-mapping) or experimentally, requires considerable effort and the results may provide limited or non-actionable mechanistic insight. In type 1 diabetes (T1D), for example, HLA*, PTPN22, INS, IFIH1* and *IL2RA* have variants with alleles with relatively large effects on risk (Odds Ratios (ORs)>1.3), and it is these loci that have yielded most biological insights so far[2-8], subsequently taken forward to translation and clinical trials[9]. As sample sizes increase even further, for example from the availability of data from large biobanks[10], loci that pass the established threshold for significance, $P < 5 \times 10^{-8}$, have either lower effect sizes or lower MAFs, the latter of which are preferable for follow-up. An alternative to typical genome-wide significance threshold is the false discovery rate (FDR)[11-13], an estimate of the probability that associations beyond a specified P value threshold are false (e.g., at FDR=0.01, 1% of associations are likely to be false).

Analyses using FDR may yield more variants associated with a trait than $P < 5 \times 10^{-8}$, providing motivation to develop a method that prioritises variants based on both significance and effect size. We define the Bigger or False Discovery Rate (BFDR) as the probability that either a variant is a false positive or that a randomly chosen true positive association exceeds it in effect size. Variables with BFDR of, for example, 5% therefore warrant greater interest than those with FDR of 5%, as they are likely to be both true positives and to exceed most other true positives in effect size. Whereas FDR=5% may be deemed too lenient for declaring an association in many settings, BFDR=5% implies both FDR<5% and a large effect, and so a BFDR 5% threshold could be used to select large effect variants that would be normally missed by a more stringent FDR threshold. This is based on the understanding that the overall cost of following up an association is a combination of a) its probability of being false and b) its probability of having an unremarkable effect size compared to other associations. Significantly,

we show that, under certain assumptions, the BFDR applies to the unobserved true effect sizes in addition to the estimated effect sizes (see SI Appendix).

Genetic variation underlying susceptibility to T1D was revealed initially in candidate gene studies, then GWAS and then fine-mapping using the custom SNP array, ImmunoChip[14-18], identifying ~50 chromosome regions associated with disease risk (https://www.opentargets.org/). Here, we apply the BFDR to discover new regions affecting T1D risk with larger effects. We performed a large GWAS meta-analysis (15,573 cases), combining two UK case-control datasets, Sardinian and Finnish case-control datasets, and families with affected offspring from the Type 1 Diabetes Genetics Consortium (T1DGC). Using SNPs outside of the HLA region, we identified 145 independently associated susceptibility regions satisfying BFDR<5% (75 not previously reported), of which 46 would have been missed by using a conventional FDR threshold of 1%. We found further associations for 74 regions satisfying FDR<1% but with BFDR>5%, which we suggest are likely to be true associations but with risk effect sizes that are likely to be difficult to follow in downstream experiments.

The common autoimmune diseases share many loci across the genome, in addition to HLA, and this overlap in genetic risk and immune pathology offers the opportunity to conduct joint analyses that may increase statistical power[18,19]. Since autoimmune thyroid disease (ATD) is very common in the UK Biobank (UKBB), with approximately 30,000 cases out of 500,000 participants, we used the BFDR and the UKBB GWAS data to map ATD associations with larger-than-average effects. We found 367 regions with BFDR<5%, of which 232 had FDR>1%. We also found 563 (60%) associated with FDR<1% but with lower effect estimates (BFDR>5%). Using colocalisation analysis, we found several T1D-associated regions that showed no evidence of effects on ATD nor with other immune diseases, suggesting that they may have roles outside of the immune system, indicative of the distinct organ-specific targets of the two diseases, i.e. the pancreatic islet beta cells (T1D) and thyroid gland (ATD). We drew on the higher power of the ATD dataset, together with pleiotropic effects of ATD variants on T1D, to identify 56 additional T1D regions (37 not previously reported) with either BFDR<5% or FDR<1% that were also ATD-associated.

Results

Bigger or False Discovery Rate (BFDR)

We searched for variants which, as is the case for *PTPN22*, *INS* and the HLA region, have large effects on T1D risk, but which might have been previously overlooked due to their low frequencies, leading to lower statistical power for detection. For this purpose we define the BFDR, for a given variant, as the overall probability that either a) the SNP is a false positive association or b) the SNP is a

true positive but randomly choosing from the distribution of true associations produce a larger effect size. The method was implemented in R. Informally, the BFDR for SNP *i* is:

$$\mathrm{BFDR}_i = \mathrm{FDR}_i + \Pr(\text{Effect of random non-null variant} > \text{Effect of SNP}_i) \times (1 - \mathrm{FDR}_i)$$

The BFDR is upper bounded by the FDR, so that all BFDRs below e.g. 1% will also have FDR<1%, and therefore applies further stringency (in terms of sizes of effects) to a set of associations passing the same FDR threshold. Here, we use BFDR<5%, which is equivalent to FDR<5% for the SNP effects estimated to be largest.

T1D GWAS meta-analysis

Imputation, QC and GWAS analysis was performed on Illumina (Infinium 550K, 3983 cases) and Affymetrix (GeneChip 500K, 1926 cases) genotyped UK samples, and on samples from Sardinia (Affymetrix 6.0 and Illumina Omni Express, 1558 cases). Affected-offspring trios from T1DGC were genotyped on the Illumina Human Core Exome beadchip and analysed with the TDT test (3173 trios) after imputation and QC. Results from the four cohorts were meta-analysed under the additive model, together with FinnGenn (4933 cases).

LD-based filtering found 219 independent T1D-associated signals (Figures 1a and 2a, Table S1a), 173 of which satisfied FDR<1% for the lead variant in the signal, with the remaining 46 having BFDR <5% in spite of having FDR>1%. We use 'independent signals' to refer to a disease-associated variant or set of variants in LD, related to, but distinct, from a physical region. These 46 variants would have been missed by using an FDR threshold of 1%, despite having a median OR of 1.19, (median MAF=4.4%) and by definition of the BFDR have FDR<5%. The 145 variants satisfying BFDR<5%, had median OR_{risk}=1.14 (median MAF=10.1%) versus 1.10 for the 173 with FDR<1% (median MAF=26.4%), indicating the shift in average effect sizes and MAF using BFDR.

Of the 219 signals, 118 can be considered 'new', being independent (r^2<0.01) from any lead variants in neither the previously most highly powered GWAS/ImmunoChip studies to date[14,18] nor in an even larger ImmunoChip study [20] (Table S1b). New signals consisted of 75 associations with BFDR<5% (median OR_{risk}=1.17, median MAF=6.5%), plus 43 with FDR<1% but BFDR>5% (median OR_{risk}=1.08, median MAF=33.5%), indicating smaller effects on risk (Tables 1a and S1b). New associations with the largest ten effect estimates are shown in Table 1a. In addition to the 75 new large effect signals, 70 out of 101 previously

reported T1D signals had BFDR<5% and 14 had BFDR<1% (*INS, PTPN22, IL2RA, MAPKAPK2* (near *FCMR*), *FKBP5* (near *DEF6*), *PGAP3* (near *IKZF3*), *SH2B3, RPS26* (near *IKZF4*), *CTRB2* (near *BCAR1*), *PTPN11, PTPN2, CTSH, APOBR* (near *IL27*) and *MEG3* (OR_{risk} ranging 1.18-1.79), highlighting the importance of their biological effects on T1D risk.

We detected 31 previously reported independent signals that were significant at FDR<1% but had BFDR>5%, implying smaller effects on risk relative to other true associations despite high confidence that they are disease-associated. Significance was at the genome-wide level ($P<5x10^{-8}$) for seven of these smaller effect associations (*PRR15L, C14orf64, IKZF1, SMARCE1* (near *CCR7*), *GATA3, IKZF3, CCDC88B*) with OR_{risk} ranging 1.09-1.10). Genome-wide significance was observed for 58 signals in total (Manhattan plot in Fig S1a), with six signals (*PRF1, RLIMP2, SLC25A37, MAGI3, LHFPL5* and *C11orf30*) not previously reported. Numbers of signals satisfying various significance criteria are summarised in Figure 3a. In total we found seven signals containing multiple conditional signals after stepwise model selection (*INS, PTPN22, IL2RA, CHD9, PTPN2*, *RLIMP2* and *AKAP11*, Table S1d).

Figure 1

Volcano plots of minor allele effect size (log odds ratio) versus significance (-log10 P values) for a) type 1 diabetes and b) autoimmune thyroid disease. All analysed SNPs are shown. SNPs with either i) Bigger or False Discovery Rate (BFDR)<5% or ii) FDR<1% were designated as associations.

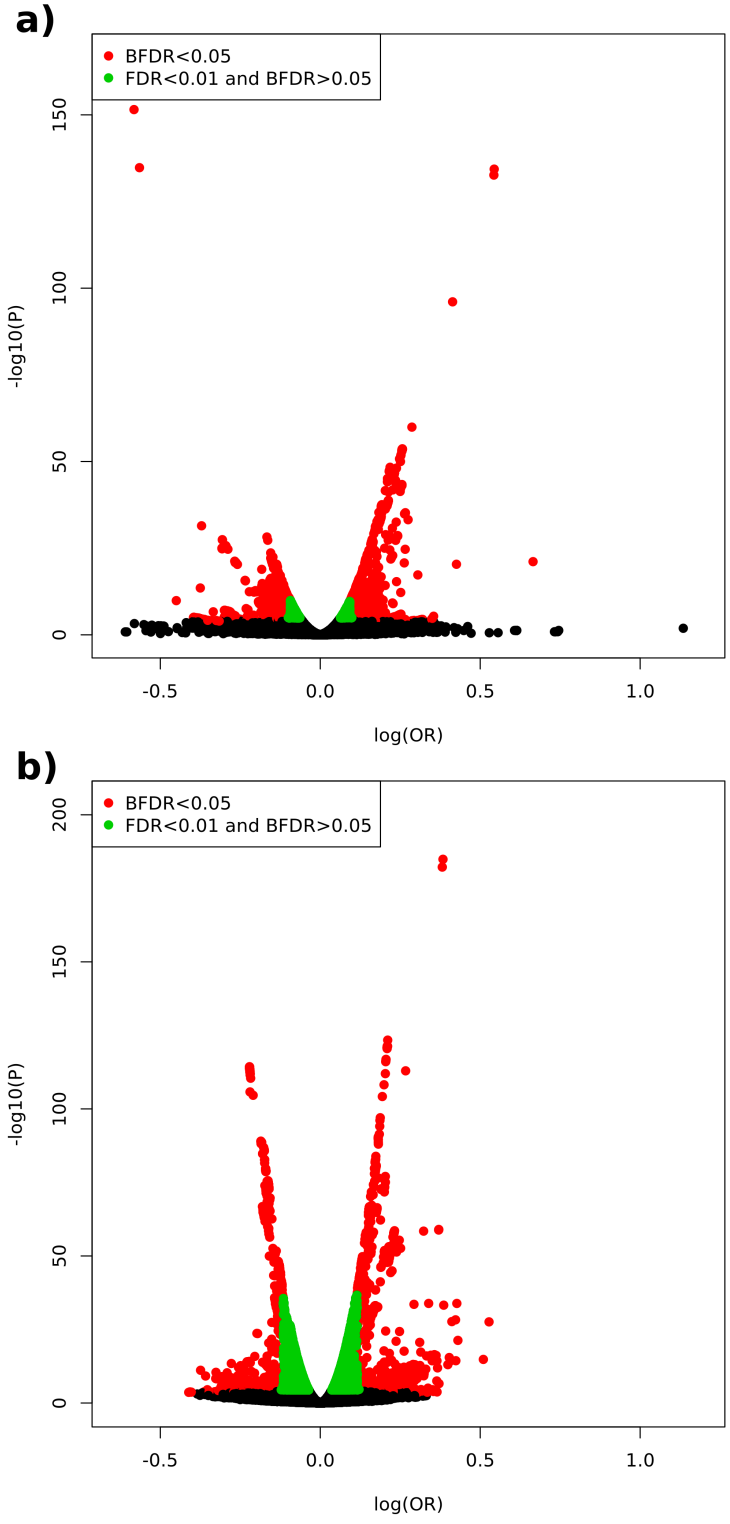

Table 1

Ten largest effect signals among a) new T1D signals and b) all ATD signals. See Tables S1-S2 for details of all associated signals. All ORs are for minor alleles. Bold regions were missed by FDR<1% but detected using BFDR<5%. IDs are for each signal's lead variant.

a)

Nearest gene	*Band*	*ID*	*MAJ*	*MIN (effect)*	*MAF**	*Imputation Info***	*P*	*OR*	*FDR*	*BFDR*	*Annotation*
RPL7P10	1p31.1	rs111551178	C	T	0.77%	97.06%	8.36E-06	0.67 (0.57-0.8)	7.09E-03	7.14E-03	intergenic
KCNJ6	21q22.13	rs75795377	T	A	0.99%	99.45%	6.36E-05	0.7 (0.59-0.84)	3.31E-02	3.32E-02	intron
RAD51D	17q12	rs28670687	T	A	0.72%	95.28%	1.74E-05	1.42 (1.21-1.67)	1.26E-02	1.27E-02	NMD transcript; non coding transcript
HORMAD1	1q21.3	rs79019274	A	T	1.05%	99.99%	6.97E-05	1.34 (1.16-1.55)	3.47E-02	3.50E-02	non coding transcript
DOCK2	5q35.1	rs113451103	T	C	2.09%	99.39%	1.19E-05	0.75 (0.65-0.85)	9.31E-03	9.69E-03	NMD transcript; non coding transcript
KIAA1715	2q31.1	rs147483205	T	A	1.37%	93.85%	8.52E-05	1.33 (1.15-1.54)	3.75E-02	3.79E-02	intron
TRIM67	1q42.2	rs148785295	G	T	1.84%	95.70%	1.10E-04	0.77 (0.67-0.88)	4.47E-02	4.54E-02	intergenic
ID4	6p22.3	rs75356149	G	T	2.33%	98.69%	1.04E-06	1.29 (1.16-1.42)	1.28E-03	2.17E-03	intergenic
TNFRSF19	13q12.12	rs138798300	A	G	1.29%	94.19%	6.36E-05	1.28 (1.13-1.45)	3.31E-02	3.40E-02	intron
NRSN1	6p22.3	rs11965813	T	A	1.30%	99.09%	1.58E-06	1.28 (1.16-1.42)	1.79E-03	2.80E-03	intergenic

*UK Illumina controls **UK Illumina all samples

b)

Nearest gene	*Band*	*ID*	*MAJ*	*MIN (effect)*	*MAF**	*Imputation Info*	*P*	*OR*	*FDR*	*BFDR*	*Annotation*
FLT3	13q12.2	rs76428106	T	C	1.29%	91.97%	1.39E-34	1.53 (1.43-1.64)	1.44E-30	7.80E-06	NMD transcript
SH3BP4	2q37.2	rs143481385	A	ATAATACATT	0.05%	91.94%	1.67E-04	0.67 (0.54-0.82)	3.26E-02	3.27E-02	regulatory region
ADCY7	16q12.1	rs78534766	C	A	0.61%	100%	3.40E-16	1.5 (1.36-1.65)	1.11E-12	1.69E-05	missense; NMD transcript; non coding transcript exon; regulatory region
PTPN22	1p13.2	rs2476601	G	A	10.25%	100%	1.33E-185	1.47 (1.43-1.51)	1.50E-178	3.20E-05	missense; 3 prime UTR; NMD transcript; non coding transcript exon
MAGI3_3	1p13.2	rs547473095	G	C	0.57%	64.56%	3.19E-08	1.44 (1.27-1.64)	2.74E-05	8.62E-05	non coding transcript
COX6CP2	20q13.13	rs73266407	G	A	0.04%	92.16%	4.09E-05	1.43 (1.2-1.69)	1.11E-02	1.11E-02	intergenic
GCG	2q24.2	rs571130497	A	G	0.57%	65.69%	3.03E-05	0.7 (0.6-0.83)	8.68E-03	8.76E-03	intergenic
CTLA4	2q33.2	rs79877750	C	T	0.90%	88.51%	4.29E-15	1.42 (1.3-1.55)	1.29E-11	9.16E-05	regulatory region
CNTNAP2_1	7q35	7:146077700_TA_T	TA	T	0.53%	41.77%	6.78E-05	1.41 (1.19-1.66)	1.66E-02	1.67E-02	non coding transcript
CYCSP42_1	21q21.1	rs2823281	A	C	0.04%	88.05%	2.12E-04	1.4 (1.17-1.67)	3.88E-02	3.90E-02	intergenic

*White Europeans

Among the new T1D signals, *RAD51D* had the third largest effect (lead variant rs28670687, P=2.12x10^{-6}, OR=1.91, MAF=0.72%), and the lead variant was in LD with three transcribed 3'UTR variants displaying evidence for being causal (fine-mapping log10 Bayes Factors 1.53) (Table S8), though they could not definitively separated from a larger credible set (log 10 Bayes factor 2.73). The chromosome region encoding its interaction partner, RAD51B, also contained a proximal T1D-associated variant, but which had a much smaller effect on risk (OR=0.92 (0.9-0.95), P=6.11x10^{-7}, FDR=8.02x10^{-4}, BFDR=0.08).

Using the two cohorts with individual genotypes available (UK Illumina and Affymetrix), we re-tested all additive associations for dominant and recessive effects at each lead variant (Table S1c). Of the 219 lead SNPs, four were most significant under a model where the minor allele was dominant (Table 2a) including *RAD51D*. No lead T1D variants were most significant under a recessive model. We repeated the GWAS analysis under both dominant and recessive models, finding 13 dominant and four recessive signals that were missed by the additive-model GWAS (independent from additive lead variants at r^2<0.05, Tables S1e-f).

Taking an alternate approach to discovery, we performed further GWAS discovery meta-analysis on four of the five cohorts (UK Illumina, UK Affymetrix, Sardinians and T1DGC), and replication analysis in the left-out Finnish cohort (FinnGen, 4933 cases and 148,190 controls), providing further evidence for large-effect signals near the *RAD51D*, and also *PRF1* (OR_{risk}=1.26 and BFDR=1.58x10^{-3}) (online methods).

Figure 2

Forest plots of lead variants in 25 largest-effect signals for a) T1D, all four cohorts used in meta-analysis, and b) ATD. Bars represent 95% confidence intervals.

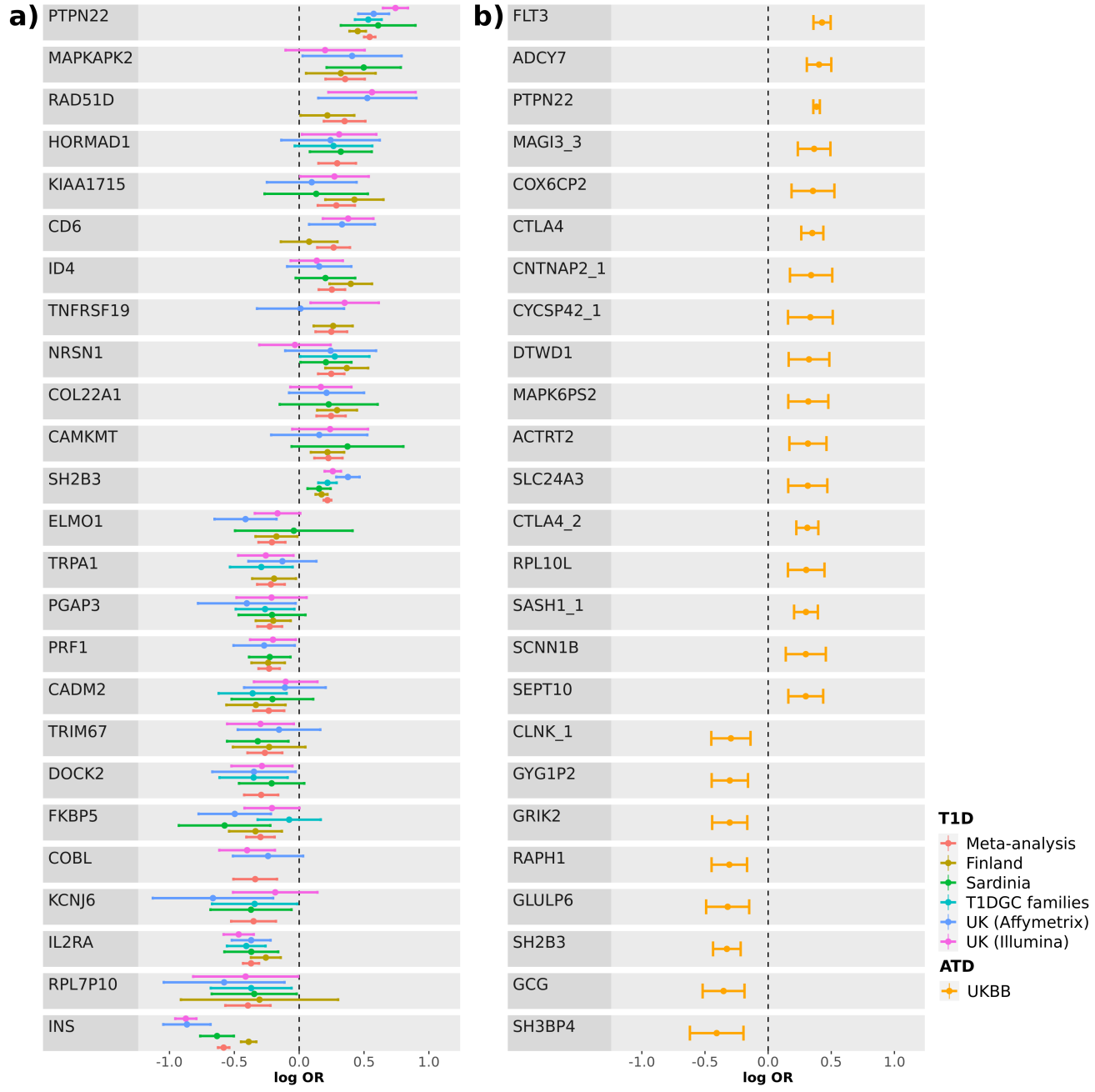

Table 2

Signals for which dominant or recessive inheritance models provided the best fits (most significant P value). IDs are for each signal's lead variant.

a) T1D signals

Nearest gene	*Band*	*ID*	*MAJ*	*MIN*	*MAF**	*Imputation info***	*P (additive)*	*OR (additive)*	*Annotation*	*OR (best model)*	*P (best model)*	*Best Model*
RAD51D	17q12	rs28670687	T	A	0.72%	95.28%	1.74E-05	1.42 (1.21-1.67)	NMD transcript; non coding transcript	1.75 (1.36-2.25)	1.50E-05	DOM
CD6	11q12.2	rs185777177	C	G	2.34%	97.92%	3.63E-05	1.3 (1.15-1.48)	intergenic	1.43 (1.23-1.67)	5.78E-06	DOM
C11orf21	11p15.5	rs756919	T	G	5.10%	95.71%	6.21E-06	1.13 (1.07-1.19)	intergenic	1.3 (1.16-1.46)	3.74E-06	DOM
TBC1D4	13q22.2	rs554648	T	G	41.02%	97.61%	1.03E-05	1.07 (1.04-1.1)	intergenic	1.24 (1.15-1.35)	6.06E-08	DOM

*UK Illumina controls **UK Illumina all samples

b) Top five largest-effect ATD signals

Nearest gene	*Band*	*ID*	*MAJ*	*MIN*	*MAF**	*Imputation Info*	*P (additive)*	*OR (additive)*	*Annotation*	*OR (best model)*	*P (best model)*	*Best model*
TGFB2	1q41	rs767491614	CAATAAATA	C	4.75%	97.30%	6.25E-07	0.9 (0.87-0.94)	intergenic	0.48 (0.37-0.63)	1.04E-07	REC
FLT3	13q12.2	rs76428106	T	C	1.29%	91.97%	1.39E-34	1.53 (1.43-1.64)	NMD transcript	1.54 (1.44-1.65)	4.79E-35	DOM
ADCY7	16q12.1	rs78534766	C	A	0.61%	100%	3.40E-16	1.5 (1.36-1.65)	missense; NMD transcript; non coding transcript exon; regulatory region	1.5 (1.36-1.65)	2.74E-16	DOM
MAGI3_3	1p13.2	rs547473095	G	C	0.57%	64.56%	3.19E-08	1.44 (1.27-1.64)	non coding transcript	1.45 (1.27-1.65)	2.09E-08	DOM
CNTNAP2_1	7q35	7:146077700_TA_T	TA	T	0.53%	41.77%	6.78E-05	1.41 (1.19-1.66)	non coding transcript	1.42 (1.2-1.68)	4.93E-05	DOM

*White Europeans

ATD GWAS in UKBB

Using 28,742 unrelated cases and 427,388 unrelated controls, we found a total of 930 ATD-associated signals (Figure 1b, Table S2a): 698 variants with FDR<1% and 367 with BFDR<5%, with median OR_{risk} of 1.07 and 1.22, respectively (median MAFs 18.5% and 0.9%). Among the 232 variants that failed to pass FDR<1% but passed BFDR<5%, the median OR_{risk} was 1.22 (median MAF 0.8%).

Previously established associations in *PTPN22, ADCY7* and *CTLA4*[21-23] have effect estimates within the largest ten (Table 1b), verifying their biological importance. The largest-effect association, *FLT3,* has a lead SNP minor allele (rs76428106 C: OR=1.53, MAF=1.29%) associated with increased monocyte count in UKBB[24]. Its importance as the largest known risk effect outside the HLA region has recently been highlighted[25]. Applying the BFDR<5% threshold, we found four additional signals with effect sizes in the top ten (Table 1b), that did not pass $P<5x10^{-8}$ or FDR<1% thresholds. The largest, *SH3BP4* (OR_{risk}=1.49, MAF=0.05%), had a 9 bp insertion as the lead and most likely causal variant (log10 Bayes Factor 2.49, see Figure S4d and Table S9 for fine-mapping results), situated within an enhancer element 2.8 Mb upstream of *AGAP1,* and is thus plausibly functional. The variant is common in Africa (e.g. 25% in HapMap Yorubans) but only present in 0.05% of white Europeans. A 5 bp insertion within the same enhancer, with almost identical effect size and MAF, also showed evidence for causality (log10 Bayes Factor 2.39).

Despite a considerable overlap in data, we detected 674 new signals that were not found in a recent UKBB ATD GWAS[23]. By including further samples not of white-European ancestry, we found 32 new signals with $P<5x10^{-8}$, but also 436 further signals using an FDR<1% threshold (Table S2b). The remaining 206 new signals were found using BFDR<5% (Figure 3b). Only three associations from the previous GWAS were further than 500 Kb from one of our lead variants, two of which we defined to be in the HLA region and thus were analysed further.

Risk ORs for the 698 variants with FDR<1% ranged from 1.04-1.53, demonstrating the high polygenicity of ATD, with many small effect associations that are detectable with large sample sizes. Genome-wide significance ($P < 5 \times 10^{-8}$) was obtained for 181 signals in total (Fig S1b). Of these, 148 (82%) had BFDR>5% (risk ORs ranging 1.05-1.12), demonstrating that most genome-wide hits are obtained for variants that we are >95% sure are either a) false associations or b) true associations with effect sizes below top 5% when ranked by size. However, BFDR analysis finds that 30/149 (20%) of previously reported genome-wide significant associations are likely to have risk effects in the top 5% (Figure 3b). Applying stepwise model selection, 36 of the 930 signals contained multiple conditional signals (Table S2d).

Testing all 930 lead SNPs under dominant and recessive inheritance models revealed 256 (28%) that were most significantly associated with dominantly acting minor alleles (Table S2c), including four of the largest-effect signals in Table 1b): *FLT3* (OR_{dom}=1.54, P_{dom}=4.79x10^{-35}), *ADCY7* (OR_{dom}=1.50, P_{dom}=2.74x10^{-16}), *MAGI3* (OR_{dom}=1.45, Pdom=2.09x10^{-8}) and *CNTNAP2_1* (OR_{dom}=1.42, P_{dom}=4.93x10^{-5}). Recessive models were most significant for nine lead SNPs (1%), eight of which had small effects under both additive and recessive models (additive OR_{risk} ranging 1.04-1.05, risk OR_{rec} ranging 1.07-1.11). One exception was *TGFB2* (rs767491614, deletion of AATAAATA), which showed a large protective recessive effect of the minor deletion allele, despite a small additive effect (OR_{rec}=0.48, P_{rec}=1.04x10^{-7}, OR_{ADD}=0.90). Details of the five largest-effect non-additive signals are shown in Table 2b. When examining genome-wide under dominant and recessive models, we detected 49 and 136 signals, respectively that were independent (r^2<0.05) from any additive lead variants (Tables S2e-f).

Figure 3

Numbers of new and previously reported signals satisfying our various significance criteria for a) type 1 diabetes and b) autoimmune thyroid disease, quantified using the lead variant in each signals.

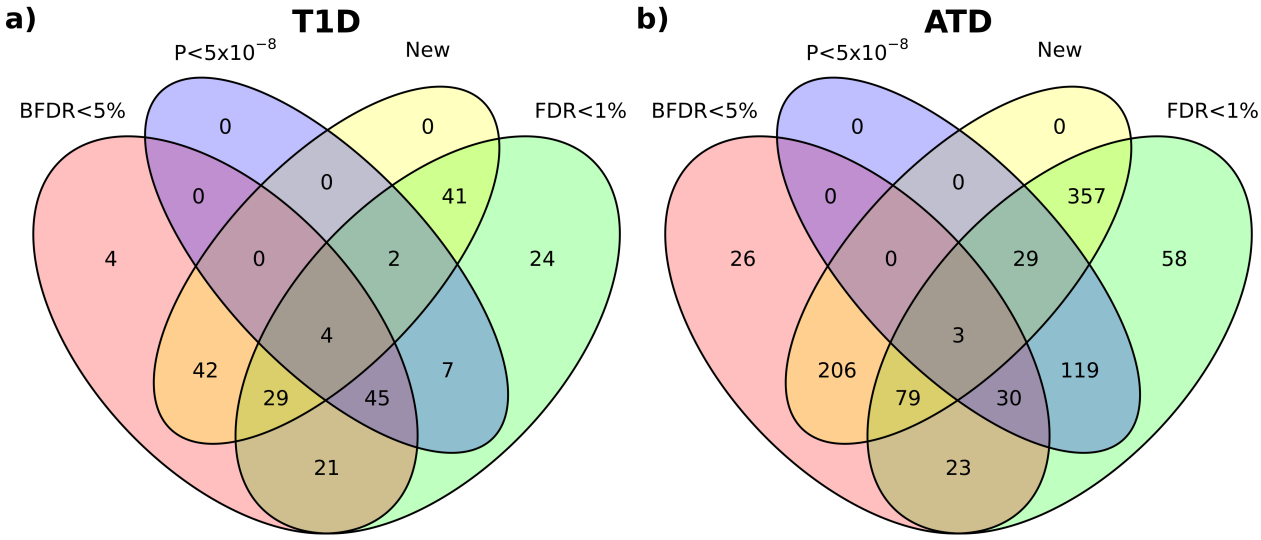

Shared and non-shared genetic causes of ATD/T1D

We define a total of 1066 independent signals from the full set of 1149 (219 T1D-defined plus 930 ATD-defined), by removing signals with lead SNPs closer than 100 Kb to a more significant lead variant in the other disease, to avoid analysing them twice, leaving 177 T1D-defined and 889 ATD-defined signals. Colocalisation analysis of the summary statistics in both phenotypes[26] found a number of signals showing strong evidence for one of four hypotheses, quantified by the corresponding posterior probabilities (PPs): a) affecting T1D only (PP_{T1D}), b) affecting ATD only (PP_{ATD}), c) separate causal associations in each dataset ($PP_{separate}$) or d) a shared causal variant (PP_{shared}). We found 19 signals with $PP_{T1D}>0.9$, and 85 with $PP_{ATD}>0.9$ (Figure 4a-b limited to the 25 with highest PP). Of these, only 3/20 $PP_{T1D}>0.9$ signals and 23/85 $PP_{ATD}>0.9$ signals were found to associate with other immune diseases in the Open Targets Genetics database (Table S10). Strong evidence for separate signals was found in 16 signals ($PP_{separate}>0.9$, Figure 4c) and shared signals in 32 signals ($PP_{shared}>0.9$, Figure 4d, limited to the 25 with highest PP_{shared}, Tables S5 and S6 for full results). Several established autoimmune loci show high evidence of shared signals, e.g. *PTPN22*, *CTLA4*, *UBASH3A* and *BACH2*. The colocalisation method assumes a single causal signal within each signal, though SNPs in LD with multiple signals' lead variants ($r^2>0.01$) were assigned to the most significant signal and excluded from others.

When both diseases share a genetic risk signal, it is possible that the risk allele for one disease is protective towards the other. We found that risk and protective alleles for the lead variants (or largest available association present in both the ATD and T1D datasets) were the same in both diseases for all 32 signals with $PP_{shared}>0.9$.

Figure 4

Posterior probabilities of colocalisation for signals with PP>0.9 for a) association with T1D only, b) with ATD only, c)separate associations for each disease within the signal d)a single association shared between the diseases within the signal. Up to the top 25 signals, ranked for maximum posterior probability, are shown in each case (full results in Tables S5 and S6). Multiple independent signals near the same gene have numerical suffixes, and the suffixes '.ATD' and '.T1D' are used when both ATD and T1D defined lead SNPs >100 Kb apart are nearest to the same gene (when lead SNPs are <100 Kb apart, these are taken to be the same signal). Posterior probabilities are truncated at 0.9 to aid visualisation.

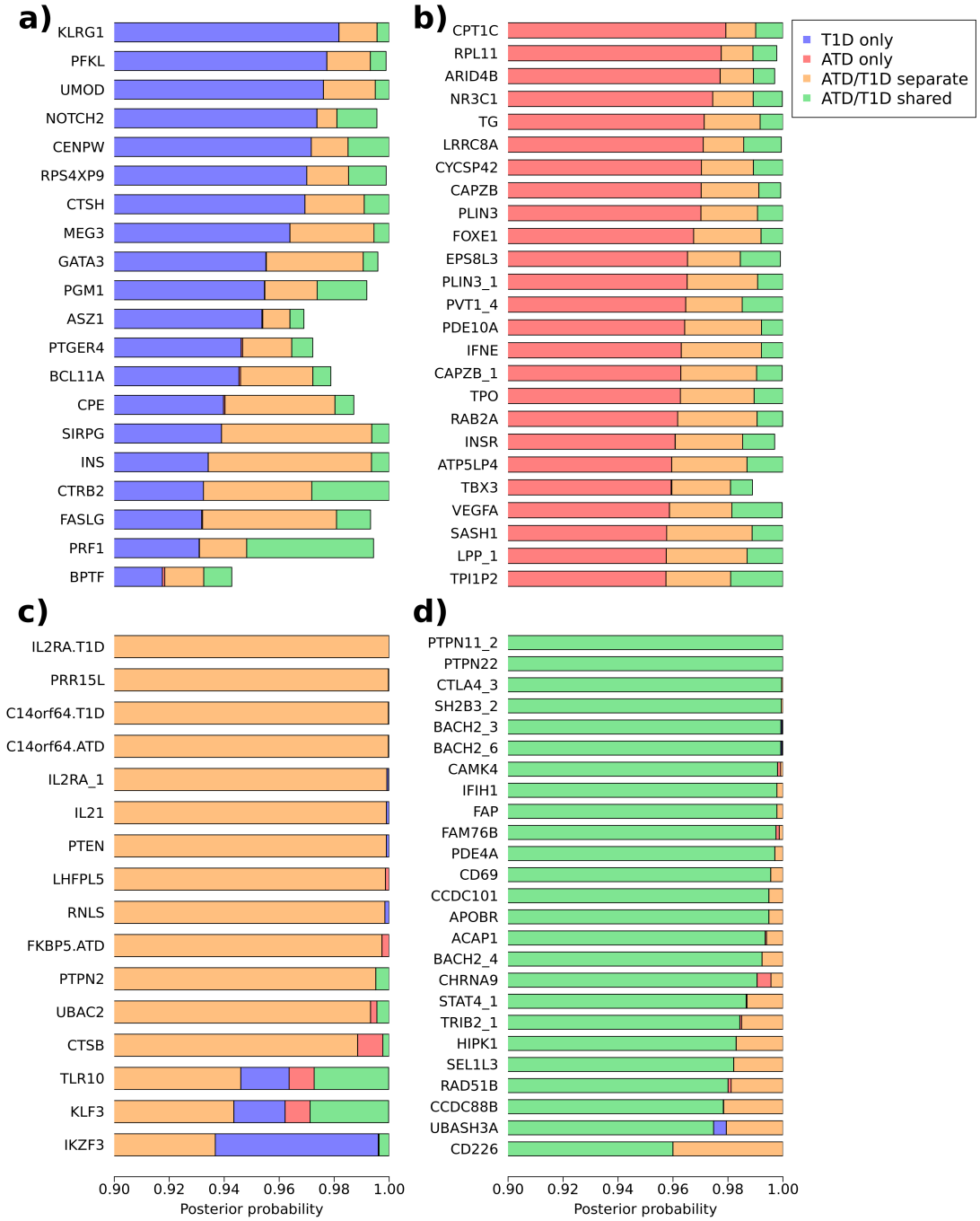

To determine the extent of shared genetic architecture between T1D and ATD, we examined the proportions of variants with high evidence for association in only one of the diseases (PP_{T1D} or PP_{ATD} > 0.9). Only 85/889 ATD signals showed some degree of ATD-only effect by this definition (PP_{ATD}>0.9, 10%), and 19/177 for T1D (PP_{T1D}>0.9, 11%). However, many signals have quite high PP for the null hypothesis of neither variant being associated (PP_{null}), with many more ATD signals showing PP_{null} > 0.33 proportionally (N_{ATD}=580/889, N_{T1D}=70/177). This is most likely due to the conservative prior probability (99.99%) assigned to the null hypothesis that a signal is not disease-associated. As local FDRs (fdrs) are empirical Bayesian estimates of the probability of zero effect for a given P value[27], we computed rescaled posterior probabilities (rsPPs) in order to maintain approximate consistency with our GWAS fdrs. Using ATD as an example, PP_{ATD}, PP_{shared} and $PP_{separate}$ can be scaled to sum to 1-fdr_{ATD}, and PP_{null} and PP_{T1D} scaled to sum to fdr_{ATD} (see online Methods). After rescaling, 102/177 T1D signals (58%) and 555/889 ATD signals (62%) showed $rsPP_{T1D/ATD}$ > 0.9 (full results in Table S7). Neither the lead ATD variants in *FLT3* or *SH3BP4,* nor any of their close LD proxies, passed QC in our T1D meta-analysis data (Figures S3e-f), so power for detecting shared signals was low, but the *FLT* variant was present in the UK Affymetrix cohort and exhibited no association with T1D (OR=1.25 (0.80-1.96)).

Of the 20 signals showing T1D-only effects using the more conservative, unscaled PPs, (PP_{T1D}>0.9, Figure 4a), *PRF1, BPTF* and *ASZ1* fell into the subset of 118 T1D-associated signals that have not been detected in previous GWAS or ImmunoChip analyses. None of these three signals had lead variants associated with other immune conditions in the Open Targets database (Table S10). *PRF1* was notable for having a larger risk effect (OR_{risk}=1.26, colocalisation plot in Figure S3b). Other large risk effect signals with high T1D specificity are the previously reported *INS* (OR=0.68) and *CTSH* (OR=0.84) (Figure 4a, Figures S3c and S3d). Despite weak evidence for T1D specificity using unscaled colocalisation PPs (PP_{T1D}=0.15, PP_{null}=0.83), *RAD51D* showed a marked difference in the appearances of signals in ATD and T1D (Figure S3a), and fdr-rescaling gave $rsPP_{T1D}$=0.96.

Colocalisation analysis suggested that power might be increased for discovering T1D associations with pleiotropic ATD effects by utilising information from the larger ATD study. There are a number of methods for jointly analysing pleiotropic phenotypes[28-31], but we took a straightforward approach by calculating BFDRs and FDRs for T1D association using only those SNPs satisfying our significance criteria in ATD (BFDR<5% or FDR<1%). These SNPs were enriched for T1D association, so the resulting BFDRs and FDRs were lower. Of the 41,561 SNPs satisfying the significance criteria in ATD (outside of the HLA region), 31,304 were present in the T1D data. An additional 56 T1D signals were

identified (r^2<0.01 with any lead variant in the primary T1D analysis), 37 of which have not been previously reported as T1D-associated. Most had small effects (ORrisk 1.05-1.12), but the one signal (*CD200R1*) had OR_{risk}=1.20 (FDR=0.04, BFDR=0.04) (Tables S3a and S3b).

Discussion

Using highly powered GWAS analyses of T1D and ATD, we detected a large number of independent genetic signals with larger effects on risk, many of which have not been associated with either disease before. Part of our success has been in identifying associations via the BFDR, a new metric for selecting associations with extreme risk effects. It is has become widely acknowledged that many, even most, variants are likely to have non-zero effects on complex phenotypes[32-34]. A large proportion of small-effect 'polygenic' risk variants are likely to be discovered in a large GWAS, especially applying thresholds on FDRs rather than conservative Bonferroni-corrected P values, exemplified by our discovery of 517 ATD risk variants at sub genome-wide significance but with FDR<1% (Figure 3b). This issue is likely to become exacerbated by the increasing availability of even larger genome-wide SNP and sequencing datasets. The BFDR is designed for selecting genetic associations for follow-up in the 'post-GWAS' era, in which the prior expectation is for there to be a very large number of small-risk associations, many with unknown biological connections to the phenotype under study. A cruder approach would be to follow-up variants that are both significant at a satisfactory FDR (e.g. <5%) and have a satisfactory effect estimate. However, thresholds on effect size will be fairly arbitrary when there is no indication of what proportion of true associations have effects that fall below it, meaning that, without more information about the distribution of effects, an OR of e.g. 1.2 could be considered either large or small.

In addition to objectively delineating variants with low FDRs but small effects on risk, we find potentially important variants for T1D and ATD with low BFDRs, but that would have been missed by an FDR<1% threshold, for example a T1D-specific signal near *RAD51D*, which encodes a DNA repair protein belonging to the *BRCA1* and *BRCA2* interacting BCDX2 complex[35]. This is supported by our finding that *RAD51B*, another BCDX2 component, is T1D- and ATD-associated, albeit with much smaller effects on risk. Three potential causal variants are in the *RAD51D* 3'UTR, implicated by fine-mapping and in high LD with the lead variant (rs28670687). Mutations in *RAD51D* are associated with ovarian cancer[36], and cells lacking *RAD51D* frequently undergo deletions of large chromosome segments, demonstrating its role in genome stability[37]. Pancreatic beta cells are long lived and non-duplicating, thus requiring high levels of genome-stability for normal functioning, and could therefore be where *RAD51D* variants lead to T1D risk, though evidence for pancreatic *RAD51D* expression is mixed[38,39]. We also detected *RAD51D* in both discovery and replication phases

when holding-out a Finnish replication cohort from our T1D meta-analysis. Using this approach, we also verified a large-effect regulatory region variant upstream of the gene for perforin (*PRF1*), which is key to the cytolytic activity of cytotoxic T-cells, and has opposite risk effects on T1D and multiple sclerosis[40], though it has no strong associations in other common diseases. Colocalisation analysis provided evidence that neither *RAD51D* nor *PRF1* signals have any strong effect on ATD.

We found a number of low frequency variants associated with larger effects on ATD, including a previously reported variant in *FLT3*, which appears to act dominantly (OR_{dom}=1.54). The minor allele is associated with both ATD risk and monocyte count[24], but has no effect on T1D. Monocytes, somewhat surprisingly, are not prioritized as a causal cell type in T1D[20] and hence this may explain why the *FLT3* variant has no effect in T1D. Mutations in *FLT3* are known to cause acute myeloid leukemia[41]. Analysing non-additive inheritance models, we also found that a deletion near *TGFB2* was associated with approximately halving ATD risk when present in two copies, though in a well-mixed population this would only affect 0.22% of individuals (MAF=4.75%). Evidence for dominant and recessive effects of minor alleles was present for approximately 28% and 1% of lead ATD variants, respectively.

A low-frequency enhancer insertion near *SH3BP4* showed a larger protective effect on ATD (OR=0.67), which is likely to be causal. The enhancer element lies in a region of few genes, but is downstream of *SH3BP*4 and upstream of *AGAP1*, either or both of which may be causal. Despite having low MAF in most populations, the protective minor allele is found in roughly 25% of West-African individuals, emphasising the requirement for more diverse GWAS datasets. Our BFDR analysis confirms the importance of 30 previously reported genome-wide significant ATD signals. In particular, signals near *ADCY7* (BFDR=1.69×10^{-5}), *PTPN22* (BFDR=3.20×10^{-5}) *MAGI3* (BFDR=8.62×10^{-5}) and *CTLA4* (BFDR=9.16×10^{-5}), are among the largest genetic risk factors. However, BFDR found that only 30/148 (20%) of previously reported genome-wide significant associations could be confirmed as having risk effects within the top 5%, suggesting the need for prioritisation of associations based on effect-size rather than on statistical significance alone.

As T1D and ATD are both autoimmune disorders, some genetic risk variants are likely to have pleiotropic effects on both disorders. As the ATD analysis in UKBB is highly powered, this provided an opportunity to leverage additional statistical power for T1D association analysis. Restricting computation of T1D FDRs and BFDRs to SNPs associated with ATD, we found 56 associations that were not significant in our primary T1D GWAS meta-analysis, though these had mostly small risk effects.

By using a conventional FDR<1% threshold in addition to BFDR<5%, we find further common (high MAF) associations for both diseases, but with smaller risk effects. The median effect size of lead SNPs with FDR<1%, i.e. those selected using significance alone, was 1.10 for T1D and 1.07 for ATD (median MAF 26.4% and 18.5%). However, this missed 46 T1D and 232 ATD variants passing BFDR<5%, with median effect sizes 1.19 and 1.22 (median MAF 4.4% and 0.80%). Associations with low FDR but small effects may be of limited importance for exploring biological hypotheses, and we recommend using a combination of effect size and significance (e.g. using the BFDR). Nevertheless, loci and common variants with smaller effects may be useful for gene-category enrichment analysis, for fitting polygenic risk scores, and for providing supporting evidence for the involvement of any larger effect variants with which they may biologically interact.

Online Methods

T1DGC data QC and GWAS analysis

Samples were obtained through the Type 1 Diabetes Genetics Consortium (T1DGC). T1DGC samples were genotyped on Illumina Human Core Exome beadchip following manufacturer protocols and genotype clusters were generated using the Illumina GeneTrain2 algorithm at University of Virginia. Since multiple array versions were used, we harmonized variants across array versions in the following way: For those SNPs that are available on the 1000 Genomes Project SNP panel, we align them to the 1000 Genomes Project SNPs separately for each array version; for those SNPs that are not available on the 1000 Genomes Project SNP panel, we harmonize them according to their positions/names, allele labels and allele frequencies that are specific to each of the four array versions.

Sample identity was confirmed by comparing genotypes from the same samples generated with an alternative array (ImmunoChip, manuscript in preparation). Variants were removed for the following reasons: a) more than 5% of genotypes were missing, b) genotypes were inconsistent across duplicates (discordant in >1% of duplicate samples or MZ twins), c) genotype frequencies deviated from Hardy Weinberg Equilibrium ($p < 1x10^{-6}$), c) Mendelian inconsistencies in more than 1% of trios or parent-offspring pairs or d) more than 10% of homozygous parent-offspring pairs or trios with heterozygous offspring. Samples were removed if more than 5% of genotypes were missing or genotypes were inconsistent with reported sex. Sample pedigree information was confirmed or corrected using genotype-inferred relationships, as determined using the software KING [42]. After QC, there were 3173 affected-offspring trios.

Subjects with European ancestry were identified for analysis using KING. Specifically, genetic principal components (PC) were generated for 1000 Genomes Phase 3 subjects and T1DGC subjects were projected onto this PC space. Then a Support Vector Machine was used to classify T1DGC subjects into one of five ancestral superpopulations, as described here http://people.virginia.edu/~wc9c/KING/kingpopulation.html. European individuals (N=10,406) were aligned to the Haplotype Reference Consortium (HRC) reference panel using available tools (https://www.well.ox.ac.uk/~wrayner/tools/index.html#Checking) and imputed to the HRC using the Michigan Imputation Server. Imputed variants were filtered for imputation quality (removed variants with imputation R-squared < 0.3) and Mendelian errors (removed variants with errors in > 1% of homozygous parent-offspring pairs or trios with heterozygous offspring). ORs were derived as OR=T/U, where T and U are the numbers of transmitted and non-transmitted alleles, and standard errors of log ORs for inverse-variance weighting were obtained following Kazeem and Farrall[43]. To prevent extreme ORs (e.g. zero or infinity), we added 0.5 to both T and U for SNPs where either value was 5 or lower.

UK T1D cohorts QC and GWAS analysis

Type 1 diabetes summary statistics were generated using GWAS data from 7977 individuals from the UK genotyped using the Illumina Infinium 550K platform (3983 cases and 3994 controls), 5268 individuals from the UK diagnosed using the Affymetrix GeneChip 500K platform (1926 cases and 3342 controls), analysed in previous publications[44,45]. We refer to these collections as 'UK Illumina' and 'UK Affymetrix'. Genotypes were imputed using the haplotype reference consortium (HRC) haplotypes for the UK collections using the Michigan Imputation server, pre phasing using SHAPEIT2 and imputation using Minimac3[46]. Variants failing either of two imputation quality criteria in either UK cohort were removed: a) imputation information score of <60% in either cases or controls, or b) difference in imputation information score between cases and controls > 1% together with MAF < 5%. An exception was made for two well-established T1D variants in the *INS-IGF2* region (rs689 and rs3842753), which were poorly imputed in the Affymetrix cohort but well imputed in the Illumina cohort. GWAS summary statistics were produced using the 'newml' method from SNPTEST, including the three largest PC covariates. Variants were LD pruned (r^2<0.3) and low (<1%) MAF SNPs removed during calculation of PCs. PCs were calculated within UK Affymetrix and Illumina collections separately.

GWAS meta-analysis of five type 1 diabetes cohorts

Summary statistics for the two UK cohorts and T1DGC were meta-analysed, together with a Sardinian cohort (1558 cases and 2882 controls, genotyped on Affymetrix 6.0 and Illumina Omni), imputed from a custom reference panel of 3,514 Sardinians[44], and samples from the FinnGen biobank resource (data freeze 4, phenotype code E4_DM1, n=4933 cases and 148,190 controls). Variants with MAF<0.5% in either UK cohort or in the Sardinian cohort were removed. SNPs not present in at least one of the UK cohorts were removed, as statistical power was likely to be low, and it is possible BFDR is unreliable for effect estimates with low precision. As the HLA region is already well established T1D-associated and has extensive linkage disequilibrium, which may interfere with downstream analysis, we removed this as standard (40,656 SNPs with build 37 positions 25-35 Mb on chromosome 6), leaving 6,254,180 SNPs.

Combined estimates of effect size from the five cohorts were obtained using inverse-variance weighting, in R:

$$\hat{\theta}_{\text{meta}} = \frac{\sum_{i=1}^{5} \hat{\theta}_i / \hat{\sigma}_i^2}{\sum_{i=1}^{5} 1/\hat{\sigma}_i^2},$$

where $\hat{\theta}_i$ is the estimate of the log OR for the *i*th cohort and $\hat{\sigma}_i^2$ its estimated standard error, which are set to zero and infinity respectively when the SNP is missing in cohort *i*. P values were computed from the meta-analysis Chi-square statistics $\hat{\theta}_{\text{meta}}^2 / \hat{\sigma}_{\text{meta}}^2$ (1 degree of freedom), where $\hat{\sigma}_{\text{meta}}^2$ is the variance of $\hat{\theta}_{\text{meta}}$:

$$\hat{\sigma}_{\text{meta}}^2 = \frac{1}{\sum_{i=1}^{5} 1/\hat{\sigma}_i^2}.$$

FDRs were calculated according to the Bejamini-Hochberg procedure[47]. Meta-analysis of dominant and recessive models was restricted to available SNPTEST results from the two UK cohorts, using the same SNPs in the additive meta-analysis. As the additive results derive from the larger five-cohort meta-analysis, the number of signals we determined to be dominant or recessive by comparing the P values of the three inheritance models is likely to be conservative.

We saw an inflation of meta-analysed Chi-square statistics (ratio of the observed median statistic over the null median of 0.456, λ_{GC} = 1.12, quantile-quantile plot in Fig S2). Analysis of the T1DGC cohort, using TDT, is immune to population

stratification. Inflation was comparable within this cohort alone (λ_{GC} = 1.09), consistent with polygenicity of T1D, rather than population stratification, being the major cause of test statistic inflation observed in the meta-analysis. Using LD-Score regression gave an estimate of 0.99 for the inflation factor due to population stratification, unbiased by the effects of polygenic association signals[48].

To assess the replicability of variants, discovery meta-analysis was performed without the inclusion of the FinnGen cohort, and replication of lead variants satisfying BFDR<5%, or FDR<1% significance criteria was performed within FinnGen. Definition of signals was performed as for the full five-cohort meta-analysis. When lead variants were not available in the replication sample, the closest LD proxy was selected using white-European LD data from UKBB. We found 184 signals in the discovery phase, of which 67 passed P<5% in the replication phase (Table S4). Replication power at P<5% was 35% for either common variants with OR=1.05 (MAF=20%) or low-frequency variants with OR=1.2 (MAF=1%)[49], assuming *D'*=0.8 and 1% T1D prevalence. Of the 184 signals, 96 were not reported in previous publications, of which 17 had lower P values after meta-analysis with the Finnish replication sample, suggesting that they are true associations. Of these, *RAD51D, PRF1, TACR1, CAMK4, AGPAT9* and *RPH3A* did not satisfy FDR<1% in the discovery phase, but were selected as discovery associations due to having BFDR<5%. *PRF1* had a larger risk effect (OR_{risk}=1.26 and BFDR=1.58x10^{-3} including FinnGen), and the lead SNP was in a regulatory region upstream of the gene, but fine-mapping could not provide evidence for any candidate causal variants within close vicinity (Figure S4b).

Autoimmune thyroid disease GWAS in UKBB

Imputed genotype data was available for 487,409 individuals and 93,095,623 autosomal variants from the UKBB, already subjected to QC. Phenotype data was available for 487,320 individuals for whom genotype was also available, and used to designate 29,045 individuals (5.96%) as ATD cases. The majority of these possessed hypothyroidism/myxedema as a non-cancer illness code (n=24,403), and 4642 additional cases were found using 'other hypothyroidism' (as distinguished from 'subclinical iodine-deficiency hypothyroidism') ICD10 main (n=67) and secondary (n=4575) codes. The various forms of hyperthyroidism were excluded from our definition of ATD as it is likely that many genetic variants have heterogeneous, possibly opposite, effects to those on hypothyroidism.

We restricted analysis to 77,675,727 autosomal SNPs with imputation information scores > 0.3. Although the UKBB genotype data has already been

subjected to QC, we removed 153,773 SNPs showing significant departure from Hardy-Weinberg Equilibrium at $P<10^{-12}$, as these probably result from poor genotype calling, and were not previously removed due via the original within-batch filtering approach[50].

We detected first and second degree relatives via IBD sharing > 25% using PLINK 2's King-robust estimator[42,51,52] and removed one random individual (n=31,190) from each pair, leaving 456,130 (28,742 cases and 427,388 controls). Relatedness was calculated using 12,788 independent autosomal variants with MAF>5% (pairwise $r^2<0.01$, pruned using PLINK).

Logistic regression models for additive risk of allele dosage on ATD were fitted for all remaining 11,261,140 autosomal SNPs outside of the HLA region with MAF>0.5%, using PLINK2. Firth regression was used instead of logistic regression for SNPs with empty contingency table cells, or when logistic regression otherwise failed to converge, as implemented in PLINK2's firth-fallback option. We controlled for population stratification using the 20 largest genetic principal components, available from UKBB, as covariates. These have been shown to reflect the broad range of ethnic backgrounds from which the participants are drawn[10], though the majority of participants are white Europeans. We also controlled for age (at initial assessment) and genotypic sex.

Chi-square statistics were inflated with $\lambda_{GC} = 1.19$, but this did not differ when controlling for the 40 largest PCs on chromosome 22. The analysis was repeated for 381,380 white European individuals (24,332 cases and 357,048 controls), identified by UKBB using a combination of self identified ethnicity and genetic ancestry PCs, giving $\lambda_{GC} = 1.18$, suggesting that inflation was primarily due to polygenic association signal rather than population stratification. LD-score regression suggested minor inflation due to population stratification, with the intercept of 1.06 suggesting that a large majority of inflation is due to polygenic signals of association, and this was similar (1.05) when using GWAS results derived from Europeans only.

Analysis of dominant and recessive effects was performed with the same covariates. To surmount computational limitations, we used PLINK2's firth-residualize approximation to firth regression[53] for analysing dominant and recessive effects across all SNPs, though firth-fallback was used to re-test the additive lead variants under recessive and dominant models.

Definition of signals

SNPs passed our significance criteria if they had FDR<0.01 and BFDR<0.05 (see SI Appendix for details on BFDR estimation). To define independent signals among this set, we selected the most significant SNP (lowest P value) on each chromosome, designating this as the lead SNP for the signal, before removing any significant variant in LD (r^2>0.01, up to maximum 1 MB distance), then choosing the next most significant SNP remaining as the lead variant for the next signal. This process ('LD clumping') was repeated until no SNPs passing our significance criteria remained. Due to the ubiquity of LD, single-SNP associations, i.e. those that have no disease-associated LD partners, are likely to be spurious due to problems with genotyping or imputation, especially when MAF is low. At each step we therefore excluded the most significant SNP from the process if it had no LD partners (r^2>0.1) with log10 P values lower than log10(P)/3-1 , where P is the lead SNP P value. LD calculations were performed in plink[54] using 381,380 individuals from the UKBB, after restricting to white-Europeans and removing first and second-degree relatives (using UKBB data field 22006). LD comparisons were restricted to a sliding window of 1 MB. The signal definition procedure was performed for each set of GWAS results separately (e.g. ATD additive, T1D additive, ATD dominant, T1D additive within ATD signals, etc). There are 47 unique previously reported T1D regions catalogued in Open Targets[1], plus another 96 in a recent ImmunoChip analysis[20]. We designated T1D signals as 'new' if they had r^2<0.05 (using the UKBB LD data) with, and were physically located at least 250kb from, the lead variants from any established regions. We used the same criteria to identify new signals for ATD, establishing lead variants' independence from 175 which were found by Kichaev et al.[23] using integration of functional enrichment information and GWAS data from UKBB hypothyroidism cases (white Europeans only), plus additional data sources[23].

Annotation of lead variants

Functional annotations for each lead variant were obtained using the biomaRt R package (Ensembl build 38 human SNP database). We also wrote command-line GraphQL and R scripts to automatically download and filter lists of immune disease pheWAS associations (P<5x10^{-5}) from the Open Targets genetics portal, for each lead variant. The diseases we filtered for were Addison's disease, asthma, celiac disease, Crohn's disease, eczema, hayfever, lupus, multiple sclerosis, psoriasis, rheumatoid arthritis, ulcerative colitis and vitiligo.

Colocalisation of genetic signals between type 1 diabetes and autoimmune thyroiditis

Colocalisation between ATD and T1D GWAS signals was performed for 500 Kb physical signals around each lead variant using the coloc package[26], after excluding variants not present in both ATD and T1D datasets. Variants having r^2>0.01 with a lead variant a more significant (lower P value) lead variant were

removed, as these probably constitute separate signals, and single-SNP associations were removed as previously described. Analysis was not possible for eight ATD-discovered signals that contained no variants present in the T1D data. LD data for coloc plots, and MAFs for coloc analysis, were computed using UKBB (white Europeans only). When lead variants in T1D and ATD discovered signals were within 100 Kb, the signal for the least significant disease (largest P value) was removed from subsequent analysis, to avoid repeating analysis of the same signals. For comparing effect sizes between each disease, we used the lead variant when this was present in both T1D and ATD datasets. Otherwise, effects were compared at the variant with the lowest P value in either disease, from all SNPs in the physical region that were present in both datasets.

Rescaling of posterior probabilities to be consistent with FDRs was performed using the local FDR (fdr) of the signal's lead variant, for the disease that it was originally discovered with. Then, taking a T1D signal as an example, the rescaled posterior probabilities (rsPPs) are:

$rsPP_{shared} = (1\text{-}fdr_{T1D}) \times PP_{shared} / (PP_{shared}+PP_{separate}+PP_{T1D})$,
$rsPP_{separate} = (1\text{-}fdr_{T1D}) \times PP_{separate} / (PP_{shared}+PP_{separate}+PP_{T1D})$,
$rsPP_{T1D} = (1\text{-}fdr_{T1D}) \times PP_{T1D} / (PP_{shared}+PP_{separate}+PP_{T1D})$,
$rsPP_{ATD} = fdr_{T1D} \times PP_{ATD} / (PP_{ATD}+PP_{null})$,
$rsPP_{null} = fdr_{T1D} \times PP_{null} / (PP_{ATD}+PP_{null})$.

This makes use of the fact that the fdr can be interpreted as an estimate of the posterior probability of no association for a given P value, and so 1-fdr is the equivalent estimate of probability of association (i.e. either a shared signal, two separate signals or a signal only at the disease in question). Local FDRs were computed following Efron & Hastie[27], using maximum likelihood estimation to fit a two-group (null and non-null) distribution to the observed Z-statistics (see SI for information about how this same process is performed as part of BFDR estimation).

Stepwise regression and Fine-mapping

Stepwise model selection was performed on GWAS summary statistics and LD data from UKBB white Europeans (n=381,380), before joint regression analysis of the selected SNPs, using COJO[55]. SNPs were incorporated into the model if they had a stepwise P value either a)lower than genome-wide significance ($P<5\times10^{-8}$) for signals where the lead variant was genome-wide significant or b)lower than the GWAS P value for the lead variant for signals where this was greater than 5×10^{-8}. Signals were defined as SNPs within 250 Kb of each lead variant, but not in LD with any more significant lead variants ($r^2>0.01$). Variants previously determined to be single-SNP associations were omitted, as described above. The

meta-analysis sample size, for each variant, was calculated as the summed sample sizes of the four case-control cohorts plus half the number of informative allele transmissions in the T1DGC TDT test. Fine-mapping for ATD and T1D was performed using FINEMAP version 1.4[56], using the GWAS summary statistics and LD data from UKBB (381,380 white Europeans). For T1D, fine-mapping was performed using the largest non-Finnish meta-analysis cohort only (UK Illumina 550K, 3983 cases and 3994 controls), to ensure homogeneity of genotyping coverage. Fine-mapping for each signal was performed using all SNPs within 500 Kb windows around the lead SNP. Due to limited statistical power, fine-mapping was not performed on the 59 additional T1D signals detected via pleiotropic effects on ATD, which have modest effects on T1D risk.

Acknowledgements

This work was funded by JDRF grants 9-2011-253 and 5-SRA-2015-130-A-N and Wellcome grants 091157 and 107212.

Computation used the Oxford Biomedical Research Computing (BMRC) facility, a joint development between the Wellcome Centre for Human Genetics and the Big Data Institute supported by Health Data Research UK and the NIHR Oxford Biomedical Research Centre. Financial support was provided by the Wellcome Trust Core Award Grant Number 203141/Z/16/Z. The views expressed are those of the author(s) and not necessarily those of the NHS, the NIHR or the Department of Health

Work was supported from grant U1301.2015/AI.1157.BE from Fondazione di Sardegna to Francesco Cucca.

We acknowledge the participants and investigators of the FinnGen study.

This research uses resources provided by the Type 1 Diabetes Genetics Consortium, a collaborative clinical study sponsored by the National Institute of Diabetes and Digestive and Kidney Diseases (NIDDK), the National Institute of Allergy and Infectious Diseases (NIAID), the National Human Genome Research Institute (NHGRI), the National Institute of Child Health and Human Development (NICHD) and JDRF and supported by grant U01 DK062418 from the US National Institutes of Health. We acknowledge the participants and members of the T1DGC (see Supplementary note for a list of members), and T1DGC steering group members Beena Akolkar, Henry A Erlich, Cécile Julier, Grant Morahan, Jørn Nerup and Concepcion Nierras.

We thank Walter Bodmer for discussions related to the BFDR method.

Author contributions

The project was conceived by J.A.T. and S.S.R.

Genotype data processing, quality control, imputation, and statistical analyses were performed by D.J.M.C., J.R.J.I, C.C.R., J-Y.Y., W-M.C., S.O.G., and C.S.

T1DGC DNA samples for genotyping were managed by S.O.G.

C.S. and F.C contributed genotype data for the Sardinian cohort

F.P. and P.C. provided samples for genotyping through their affiliated institutions and research programs.

Biological interpretation of results was provided by A.J.C and J.A.T.

The manuscript was written by D.J.M.C. (under supervision by J.A.T.) with additional material from J.R.J.I. and C.C.R.

Competing interests

No authors have any competing interests to declare.

References

1 Carvalho-Silva, D. *et al.* Open Targets Platform: new developments and updates two years on. *Nucleic Acids Res* **47**, D1056-D1065, doi:10.1093/nar/gky1133 (2019).

2 Dendrou, C. A. *et al.* Cell-specific protein phenotypes for the autoimmune locus IL2RA using a genotype-selectable human bioresource. *Nat Genet* **41**, 1011-1015, doi:10.1038/ng.434 (2009).

3 Downes, K. *et al.* Reduced expression of IFIH1 is protective for type 1 diabetes. *PLoS One* **5**, doi:10.1371/journal.pone.0012646 (2010).

4 Ferreira, R. C. *et al.* Chronic Immune Activation in Systemic Lupus Erythematosus and the Autoimmune PTPN22 Trp(620) Risk Allele Drive the Expansion of FOXP3(+) Regulatory T Cells and PD-1 Expression. *Front Immunol* **10**, 2606, doi:10.3389/fimmu.2019.02606 (2019).

5 Garg, G. *et al.* Type 1 diabetes-associated IL2RA variation lowers IL-2 signaling and contributes to diminished CD4+CD25+ regulatory T cell function. *J Immunol* **188**, 4644-4653, doi:10.4049/jimmunol.1100272 (2012).

6 Smyth, D. J. *et al.* PTPN22 Trp620 explains the association of chromosome 1p13 with type 1 diabetes and shows a statistical interaction with HLA class II genotypes. *Diabetes* **57**, 1730-1737, doi:10.2337/db07-1131 (2008).

7 Todd, J. A. *et al.* Regulatory T Cell Responses in Participants with Type 1 Diabetes after a Single Dose of Interleukin-2: A Non-Randomised, Open Label, Adaptive Dose-Finding Trial. *PLoS Med* **13**, e1002139, doi:10.1371/journal.pmed.1002139 (2016).

8 Vafiadis, P. *et al.* Insulin expression in human thymus is modulated by INS VNTR alleles at the IDDM2 locus. *Nat Genet* **15**, 289-292, doi:10.1038/ng0397-289 (1997).

9 Marcovecchio, M. L. *et al.* Interleukin-2 Therapy of Autoimmunity in Diabetes (ITAD): a phase 2, multicentre, double-blind, randomized, placebo-controlled trial. *Wellcome Open Res* **5**, 49, doi:10.12688/wellcomeopenres.15697.1 (2020).

10 Bycroft, C. *et al.* The UK Biobank resource with deep phenotyping and genomic data. *Nature* **562**, 203-209, doi:10.1038/s41586-018-0579-z (2018).

11 Stephens, M. False discovery rates: a new deal. *Biostatistics* **18**, 275-294, doi:10.1093/biostatistics/kxw041 (2016).

12 Brzyski, D. *et al.* Controlling the Rate of GWAS False Discoveries. *Genetics* **205**, 61-75, doi:10.1534/genetics.116.193987 (2017).

13 Benjamini, Y. & Yekutieli, D. Quantitative trait Loci analysis using the false discovery rate. *Genetics* **171**, 783-790, doi:10.1534/genetics.104.036699 (2005).

14 Barrett, J. C. *et al.* Genome-wide association study and meta-analysis find that over 40 loci affect risk of type 1 diabetes. *Nat Genet* **41**, 703-707, doi:10.1038/ng.381 (2009).

15 Bradfield, J. P. *et al.* A genome-wide meta-analysis of six type 1 diabetes cohorts identifies multiple associated loci. *PLoS Genet* **7**, e1002293, doi:10.1371/journal.pgen.1002293 (2011).

16 Todd, J. A. *et al.* Robust associations of four new chromosome regions from genome-wide analyses of type 1 diabetes. *Nat Genet* **39**, 857-864, doi:10.1038/ng2068 (2007).

17 Wellcome Trust Case Control Consortium. Genome-wide association study of 14,000 cases of seven common diseases and 3,000 shared controls. *Nature* **447**, 661-678, doi:10.1038/nature05911 (2007).

18 Onengut-Gumuscu, S. *et al.* Fine mapping of type 1 diabetes susceptibility loci and evidence for colocalization of causal variants with lymphoid gene enhancers. *Nat Genet* **47**, 381-386, doi:10.1038/ng.3245 (2015).

19 Fortune, M. D. *et al.* Statistical colocalization of genetic risk variants for related autoimmune diseases in the context of common controls. *Nat Genet* **47**, 839-846, doi:10.1038/ng.3330 (2015).

20 Robertson, C. C. *et al.* Fine-mapping, trans-ancestral and genomic analyses identify causal variants, cells, genes and drug targets for type 1 diabetes. *bioRxiv*, 2020.2006.2019.158071, doi:10.1101/2020.06.19.158071 (2020).

21 de Lange, K. M. *et al.* Genome-wide association study implicates immune activation of multiple integrin genes in inflammatory bowel disease. *Nat Genet* **49**, 256-261, doi:10.1038/ng.3760 (2017).

22 Stahl, E. A. *et al.* Genome-wide association study meta-analysis identifies seven new rheumatoid arthritis risk loci. *Nat Genet* **42**, 508-514, doi:10.1038/ng.582 (2010).

23 Kichaev, G. *et al.* Leveraging Polygenic Functional Enrichment to Improve GWAS Power. *Am J Hum Genet* **104**, 65-75, doi:10.1016/j.ajhg.2018.11.008 (2019).

24 Astle, W. J. *et al.* The Allelic Landscape of Human Blood Cell Trait Variation and Links to Common Complex Disease. *Cell* **167**, 1415-1429 e1419, doi:10.1016/j.cell.2016.10.042 (2016).

25 Saevarsdottir, S. *et al.* FLT3 stop mutation increases FLT3 ligand level and risk of autoimmune thyroid disease. *Nature* **584**, 619-623, doi:10.1038/s41586-020-2436-0 (2020).

26 Giambartolomei, C. *et al.* Bayesian test for colocalisation between pairs of genetic association studies using summary statistics. *PLoS Genet* **10**, e1004383, doi:10.1371/journal.pgen.1004383 (2014).

27 Efron, B. & Hastie, T. *Computer age statistical inference : algorithms, evidence, and data science*. (Cambridge University Press, 2016).

28 Liley, J. & Wallace, C. A pleiotropy-informed Bayesian false discovery rate adapted to a shared control design finds new disease associations from GWAS summary statistics. *PLoS Genet* **11**, e1004926, doi:10.1371/journal.pgen.1004926 (2015).

29 Liley, J. & Wallace, C. Accurate error control in high dimensional association testing using conditional false discovery rates. *bioRxiv*, 414318, doi:10.1101/414318 (2019).

30 Andreassen, O. A. *et al.* Improved detection of common variants associated with schizophrenia and bipolar disorder using pleiotropy-informed conditional false discovery rate. *PLoS Genet* **9**, e1003455, doi:10.1371/journal.pgen.1003455 (2013).

31 O'Reilly, P. F. *et al.* MultiPhen: joint model of multiple phenotypes can increase discovery in GWAS. *PLoS One* **7**, e34861, doi:10.1371/journal.pone.0034861 (2012).

32 Crouch, D. J. M. & Bodmer, W. F. Polygenic inheritance, GWAS, polygenic risk scores, and the search for functional variants. *Proc Natl Acad Sci U S A* **117**, 18924-18933, doi:10.1073/pnas.2005634117 (2020).

33 Boyle, E. A., Li, Y. I. & Pritchard, J. K. An Expanded View of Complex Traits: From Polygenic to Omnigenic. *Cell* **169**, 1177-1186, doi:10.1016/j.cell.2017.05.038 (2017).

34 O'Connor, L. J. The distribution of common-variant effect sizes. *bioRxiv*, 2020.2009.2019.304097, doi:10.1101/2020.09.19.304097 (2020).

35 Masson, J. Y. *et al.* Identification and purification of two distinct complexes containing the five RAD51 paralogs. *Genes Dev* **15**, 3296-3307, doi:10.1101/gad.947001 (2001).

36 Loveday, C. *et al.* Germline mutations in RAD51D confer susceptibility to ovarian cancer. *Nat Genet* **43**, 879-882, doi:10.1038/ng.893 (2011).

37 Reh, W. A., Nairn, R. S., Lowery, M. P. & Vasquez, K. M. The homologous recombination protein RAD51D protects the genome from large deletions. *Nucleic Acids Res* **45**, 1835-1847, doi:10.1093/nar/gkw1204 (2017).

38 G. TEx Consortium. Human genomics. The Genotype-Tissue Expression (GTEx) pilot analysis: multitissue gene regulation in humans. *Science* **348**, 648-660, doi:10.1126/science.1262110 (2015).

39 Wang, D. *et al.* A deep proteome and transcriptome abundance atlas of 29 healthy human tissues. *Mol Syst Biol* **15**, e8503, doi:10.15252/msb.20188503 (2019).

40 Sidore, C. *et al.* PRF1 mutation alters immune system activation, inflammation, and risk of autoimmunity. *Multiple Sclerosis Journal* **0**, 1352458520963937, doi:10.1177/1352458520963937.

41 Baldus, C. D., Mrozek, K., Marcucci, G. & Bloomfield, C. D. Clinical outcome of de novo acute myeloid leukaemia patients with normal cytogenetics is affected by molecular genetic alterations: a concise review. *Br J Haematol* **137**, 387-400, doi:10.1111/j.1365-2141.2007.06566.x (2007).

42 Manichaikul, A. *et al.* Robust relationship inference in genome-wide association studies. *Bioinformatics* **26**, 2867-2873, doi:10.1093/bioinformatics/btq559 (2010).

43 Kazeem, G. R. & Farrall, M. Integrating case-control and TDT studies. *Ann Hum Genet* **69**, 329-335, doi:10.1046/j.1529-8817.2005.00156.x (2005).

44 Inshaw, J. R. J. *et al.* Divergent genetic effects for type 1 and type 2 diabetes at overlapping association signals. *bioRxiv*, 2020.2006.2017.156778, doi:10.1101/2020.06.17.156778 (2020).

45 Cooper, N. J. *et al.* Type 1 diabetes genome-wide association analysis with imputation identifies five new risk regions. *bioRxiv*, 120022, doi:10.1101/120022 (2017).

46 Das, S. *et al.* Next-generation genotype imputation service and methods. *Nat Genet* **48**, 1284-1287, doi:10.1038/ng.3656 (2016).

47 Benjamini, Y. & Hochberg, Y. Controlling the False Discovery Rate - a Practical and Powerful Approach to Multiple Testing. *J Roy Stat Soc B Met* **57**, 289-300 (1995).

48 Bulik-Sullivan, B. K. *et al.* LD Score regression distinguishes confounding from polygenicity in genome-wide association studies. *Nat Genet* **47**, 291-295, doi:10.1038/ng.3211 (2015).

49 Purcell, S., Cherny, S. S. & Sham, P. C. Genetic Power Calculator: design of linkage and association genetic mapping studies of complex traits. *Bioinformatics* **19**, 149-150, doi:10.1093/bioinformatics/19.1.149 (2003).

50 Kanai, M., Howrigan, D., Daly, M. & Finucan, H. (2019).

51 Chang, C. C. *et al.* Second-generation PLINK: rising to the challenge of larger and richer datasets. *Gigascience* **4**, 7, doi:10.1186/s13742-015-0047-8 (2015).

52 Purcell, S. M. & Chang, C. C. *PLINK 2.0.,* http://www.cog-genomics.org/plink/2.0/.

53 Mbatchou, J. *et al.* Computationally efficient whole genome regression for quantitative and binary traits. *bioRxiv*, 2020.2006.2019.162354, doi:10.1101/2020.06.19.162354 (2020).

54 Purcell, S. *et al.* PLINK: a tool set for whole-genome association and population-based linkage analyses. *Am J Hum Genet* **81**, 559-575, doi:10.1086/519795 (2007).

55 Yang, J. *et al.* Conditional and joint multiple-SNP analysis of GWAS summary statistics identifies additional variants influencing complex traits. *Nat Genet* **44**, 369-375, S361-363, doi:10.1038/ng.2213 (2012).

56 Benner, C. *et al.* FINEMAP: efficient variable selection using summary data from genome-wide association studies. *Bioinformatics* **32**, 1493-1501, doi:10.1093/bioinformatics/btw018 (2016).